

Screening of Different *Fusarium* Species to Select Potential Species for the Synthesis of Silver Nanoparticles

Swapnil C. Gaikwad,^a Sonal S. Birla,^a Avinash P. Ingle,^a Aniket K. Gade,^{a,e}
Priscyla D. Marcato,^{b,c} Mahendra Rai^{*,a,c} and Nelson Duran^{c,d}

^aDepartment of Biotechnology, SGB Amravati University, Amravati-444 602, Maharashtra, India

^bInstitute of Chemistry, Biological Chemistry Laboratory, Universidade Estadual de Campinas, CP 6154, 13083-970 Campinas-SP, Brazil

^cNanobiolab, Faculty of Pharmaceutical Sciences of Ribeirão Preto, Universidade de São Paulo, Av. do Café, s/n, 14040-903 Ribeirão Preto-SP, Brazil

^dCenter of Natural and Human Sciences, Universidade Federal do ABC, Rua Santa Adélia, 166, 09210-170 Santo André-SP, Brazil

^eDepartment of Biology, Utah State University, 84322 Logan-UT, USA

Onze diferentes espécies de *Fusarium* foram isoladas a partir de vários materiais vegetais infectados e selecionados para escolher uma espécie potencialmente importante para a síntese de nanopartículas de prata. Todos os isolados foram identificados com base nas características de cultivo e microscópicas usando as chaves de identificação de *Fusarium*. Para a confirmação e identificação preliminar dos isolados de espécies de *Fusarium*, a análise BLAST on-line foi utilizada. Das espécies isoladas onze mostraram a capacidade para a síntese de nanopartículas de prata. A síntese de nanopartículas de prata foi confirmada por espectroscopia de UV-Vis que mostrou um pico característico em torno de 420 nm. Além disso, a confirmação da síntese de nanopartículas de prata foi realizada utilizando a análise de rastreamento de nanopartículas (nanoparticle tracking analysis-NTA), medidas de potencial zeta, espectroscopia de correlação de fótons (PCS), difratometria de raios X de pó (XRD), e microscopia eletrônica de transmissão (TEM). As menores nanopartículas de prata foram sintetizadas por *F. oxysporum* (3-25 nm), enquanto as maiores foram obtidas com *F. solani* (3-50 nm).

Eleven different *Fusarium* species were isolated from various infected plant materials and screened to select a potential species for the synthesis of silver nanoparticles. All the isolates were identified on the basis of cultural and microscopic characteristics using *Fusarium* identification keys. For the confirmation of preliminary identified isolates of *Fusarium* species, online BLAST analysis was carried out. All the eleven species demonstrated the ability for synthesis of silver nanoparticles. This was confirmed by UV-Vis spectroscopy, which gave characteristic peak around 420 nm. Further confirmation of silver nanoparticles was carried out using nanoparticles tracking analysis (NTA), zeta potential, photon correlation spectroscopy (PCS), powder X-ray diffractometry (XRD) and transmission electron microscopy (TEM). The smallest size of silver nanoparticles was synthesized by *F. oxysporum* (3-25 nm) and largest size silver nanoparticles were synthesized by *F. solani* (3-50 nm).

Keywords: silver nanoparticles, *Fusarium*, NTA, zeta potential, TEM

Introduction

Nanotechnology is a multidisciplinary field linked with different disciplines of science and technology like

biology, chemistry, physics and engineering. It is the most fascinating branch of material science, which has ability to deal with the physical and chemical properties of materials by creating novel tiny structures with fundamentally novel properties and better functioning. These nanomaterials possess those desired features, which overcome the difficulties came across while dealing with the bulk

*e-mail: gaikwad.swapnil1@gmail.com, mkrai123@rediffmail.com, pmkrai@hotmail

materials. Nanotechnology works with the measured scale between individual molecules and 100 nanometer where materials possess different properties than bulk materials. Nanomaterials are helpful in solving the problems of technology related to electronics,¹ energy,² environment,³ pharmacology, medicine⁴ and agriculture science^{5,6} up to certain extent. One of the most valuable creations of nanotechnology is the metal nanoparticles, which form the basis of nanomaterials. Nowadays, the synthesis of nanoparticles is a fascinating area of research due to their unique physical,⁷ chemical,⁸ catalytic,⁹ opto-electronic¹⁰ properties and most importantly their larger surface area-to-volume ratio. In fact, the development of reliable green protocols for the synthesis of nanoparticles over a range of chemical composition, size and high monodispersity are the challenging issues.¹¹ Chemical and physical synthesis methods of nanoparticles are capital-intensive, include toxic chemicals and show low bioactivity compared to biogenic synthesis. Therefore, the need for clean, eco-friendly, cost-effective and biocompatible synthesis of metal nanoparticles encouraged the researchers to utilize the biological resources as nanofactory. There are many reports of biosynthesis of metallic nanoparticles by using different prokaryotic microbes like bacteria¹² and eukaryotic cell system including actinomycetes,¹³ yeasts,^{14,15} algae,^{16,17} plants¹⁸ and fungi.¹⁹⁻²⁶ Rai *et al.*²⁷ proposed the term “Myconanotechnology” for the research carried out on nanoparticles synthesis by fungal system. It is the interface between mycology and nanotechnology. Many fungi have the ability to produce different nanoparticles like silver,^{28,29} gold, platinum,³⁰ cadmium sulfide,^{31,32} zirconia, silica,^{33,34} titanium,³⁵ etc. Moreover, among different metal nanoparticles such as copper, iron and their oxides, silver nanoparticles are most attractive choice due to their multiple applications in food preservation,³⁶ textile,³⁷⁻³⁹ cosmetics,⁴⁰ plant tissue culture,⁴¹ water purification,⁴² medical science such as dental materials,⁴³⁻⁴⁵ coating stainless steel in medical devices⁴⁶ and as potential antimicrobial and antimalarial agents.⁴⁷

So far, many fungi have been exploited for the synthesis of silver nanoparticles. It has been found that among all the biosystems, fungi have many advantages over the other systems because of their high tolerance towards the heavy metals, easy and simple scale-up method, easy biomass handling, recovery and economic viability.^{24,25,34} Moreover, the synthesis being extracellular reduces the downstream processing cost. Hence, among all the biosystems, fungal system is the best for the biosynthesis of nanoparticles. Since antiquity, silver metal has been used in different ways such as, utensils and ornaments due to its unique

antimicrobial nature. In addition, for centuries, silver in different forms such as silver nitrate, silver sulfadiazine, etc. has been used to treat the burns and chronic wounds sepsis, venereal diseases, perianal abscesses and in dental materials due to its antimicrobial properties while silver zeolite is used for surface coating to apply antimicrobial property to the materials, which are used for food preservation and disinfection of medical devices. Nanotechnology enhances the antimicrobial potential of silver by shaping it to nanoparticles. In this respect, they appear to be novel antimicrobial agents even against multi-drug resistant microorganisms.^{24,48-50}

In the present study, we screened 11 different *Fusarium* species for the selection of species having high potential for the synthesis of silver nanoparticles.

Experimental

Isolation of different *Fusarium* species

Infected plant materials such as fruits, vegetable and food grains were collected from different places of India. *Fusarium* species were isolated from these materials on potato dextrose agar and incubated at 28 °C. These isolates were cultured, purified and maintained on potato dextrose agar (PDA) at 4 °C. Later, all the isolates were identified on the basis of cultural characteristics (type and growth rate of mycelia, dorsal and ventral colour of the colony, etc.), and microscopic characteristics (presence or absence of conidia, size of conidia, shape and septation of macroconidia, etc.) using *Fusarium* identification keys.^{51,52} Further, the identity of different *Fusaria* sp. was confirmed by ITS-rDNA sequence comparison.

Identification of *Fusarium* sp.

ITS-rDNA regions of 11 *Fusarium* species (one representative species from each of all 11 groups identified on the basis of morphological characters) were amplified by PCR using the primers ITS1 (5'-TCCGTAGGTGAACCTGCGG3') and ITS4 (5'-TCCTCCGCTTATTGATATGC-3') designed and synthesized from Chromous Biotech Pvt. Ltd, Bangalore, India. Each PCR reaction mixture contained, 2X PCR master mix (12.5 µL) (Fermentas Life Sciences, Canada), genomic DNA (5 µL), 1 µmol L⁻¹ each of the primers ITS1 and ITS4 (1 µL), 25 mmol L⁻¹ MgCl₂ (1.5 µL) (provided with PCR master mix) additional Taq DNA polymerase (0.3 µL) (Genaxy, 5 U µL⁻¹) and nuclease free distilled water (3.7 µL) (supplied with Fermentas PCR master mix) in a total volume of 25 µL.

PCR was carried out on gradient PCR machine (Palm-Cycler from Corbett Research, Australia) and thermal cycler (Eppendorf, Germany). The programme included the same conditions used for the amplification of DNA for RAPD. It includes initial denaturation at 94 °C for 2 min, 35 cycles with denaturation at 94 °C for 30 sec, annealing 38 °C for 1 min, extension at 72 °C for 2 min and final extension at 72 °C for 5 min with holding temperature at 4 °C for 10 min. Negative control (without template DNA) was maintained for each set of experiment to test for the presence of non-specific banding. All experiments were repeated for three times. PCR products were electrophoresed on 1.5 % agarose by using 1X TAE buffer (Fermentas Life Sciences, Canada), stained with ethidium bromide, visualised in a UV-transilluminator and the gel were photographed using Gel Doc system (AlphaImager, Gel documentation system, USA). After proper amplification PCR products were sent for sequencing to Chromous Biotech Pvt. Ltd, Bangalore, India.

For the confirmation of preliminary identified isolates of *Fusarium* species, online Basic Local Alignment Search Tool (BLAST) analysis was carried out. After sequencing, ITS sequences were added into the test sequence window at online BLAST program, which provided results in the form of best matches with the available sequences in GeneBank.

Unweighted Pair Group Method with Arithmetic Mean analysis (UPGMA) was carried out from the ITS r-DNA sequences obtained to find out the similarity between each *Fusarium* species. The Numerical Taxonomy System of Multivariate Statistical Programme (NTSYS) software package was used to get the phenotypic cluster and phylogenetic tree stating the genetic relationship among the different species of *Fusarium*.

Synthesis of silver nanoparticles using *Fusarium* species

All the *Fusarium* species were inoculated in 250 mL Erlenmeyer flasks each containing 100 mL of potato dextrose broth (PDB) and later incubated at 26 ± 2 °C for 5-7 days. Mycelia thus grown were harvested by filtration through Whatman filter paper No.1 and thrice washed with autoclaved distilled water. Harvested mycelia were resuspended in 100 mL autoclaved distilled water and incubated at room temperature for 24 hrs. After incubation mycelia were collected by filtration through Whatman filter paper No.1 and the fungal debris was removed by centrifugation. Thereafter, the filtrates were treated with 1 mmol L⁻¹ AgNO₃ and kept at room temperature for complete reduction. Only fungal cell filtrate (without treatment with 1 mmol L⁻¹ AgNO₃) as positive control and 1 mmol L⁻¹ AgNO₃ as negative control were maintained. All the experiments were performed in triplicate.

Characterization of Silver Nanoparticles

UV- Visible Spectroscopy Analysis

The formation of silver nanoparticles was confirmed by the presence of plasmon band and analysed by UV-Visible spectrophotometer (Shimadzu-UV 1700, Japan) at resolution of 1 nm and scanning the absorbance spectra in 200-800 nm range of wavelength.

Nanoparticle Tracking Analysis (NTA)

The size of synthesized nanoparticles was measured by Nanosight (LM-20, UK) using Nanoparticle Tracking and Analysis (NTA-2.0) software. NTA gives the size distribution of nanoparticles, which can be traced out using particles by particles analysis. NTA depends upon the brownian movement of the nanoparticles. For the analysis, samples were diluted with the nuclease free water and 0.5 mL of diluted sample was injected onto the sample chamber and observed through LM 20 to measure the size of the nanoparticles.

Zeta potential measurement analysis

Surface charges acquired by nanoparticles in medium were measured by ZetaSizer instrument (Malvern Instruments Corp, UK) at 25 °C in polystyrene cuvettes with path length of 10 mm. The average nanoparticle size distribution was also measured by ZetaSizer (size by number) (Malvern Instruments Corp, UK).

Powder X-ray diffractometry (XRD)

The crystalline nature of silver nanoparticles was determined by powder X-ray diffractometry (XRD- XD3A, Shimadzu, Japan) equipped with nickel-filtered Cu-K α radiation (40 KV, 30 mA) at an angle of 2 θ from 5° to 50°. The scan speed was 0.02 degree / min and the time constant was 2 s. The particle size (Diameter D) was calculated from XRD peaks according to Scherrer's equation:

$$D = (K\lambda) / (\beta_{cor} \cos\theta), \text{ with } \beta_{cor} = (\beta_{sample}^2 - \beta_{ref.}^2)^{1/2}$$

where D is the average crystal size, K is Scherrer's coefficient (0.89), λ is the X-ray wavelength ($\lambda = 1.542 \text{ \AA}$), θ is Bragg's angle ($2\theta = 25.1^\circ$), β_{cor} is the correction of the full width at half-maximum (FWHM) in radians, and β_{sample} and $\beta_{ref.}$ are the FWHM of the reference and sample peaks, respectively.

Transmission Electron Microscopy (TEM)

To determine the size and morphological variation of silver nanoparticles synthesized by different *Fusaria* species, the TEM analysis was carried out using Carl Zeiss

CEM-902 (80 KeV). For the examination of the silver nanoparticles, one drop of the particle dispersion diluted was deposited on carbon coated parlodion films supported in 300 mesh copper grids (Ted Pella).

Results and Discussion

We isolated eleven different *Fusarium* species from infected fruits, vegetables and food grains. These species were identified on the basis of cultural characteristics (type of mycelia, growth rate, dorsal and ventral colour of colony, etc.) and microscopic characteristics (presence or absence of conidia, size of conidia, septation in macroconidia, shape of macroconidia, etc.) using *Fusarium* identification keys.^{51,52} *Fusarium* species produced three types of spores, i.e., microconidia, macroconidia and chlamyospores.⁵³ However, the presence of macroconidia is the most important characteristic that distinguishes *Fusarium* from other genera. Macroconidia are formed in sporodochium with shape of a moon crest (sickle shape) or a boat or banana with multiseptum.⁵⁴ Cultural and microscopic characteristics confirmed the identity of 11 different species of *Fusarium* viz., *F. graminearum*, *F. solani*, *F. oxysporum*, *F. culmorum*, *F. scirpi*, *F. tricinctum*, *F. acuminatum*, *F. semitectum*, *F. proliferatum*, *F. equiseti*, *F. moniliforme*. Further confirmation of these species was based on ITS-rDNA sequence comparison with available sequences in the data base (NCBI) using online BLAST analysis programme.

For ITS-rDNA analysis, DNA of 11 *Fusarium* species, namely *F. semitectum*, *F. solani*, *F. oxysporum*, *F. equiseti*, *F. acuminatum*, *F. scirpi*, *F. proliferatum*, *F. tricinctum*, *F. moniliforme*, *F. graminearum* and *F. culmorum* was isolated and ITS regions were amplified using species -specific primers ITS1 (5'-TCCGTAGGTGAACCTGCGG-3') and ITS4 (5'-TCCTCCGCTTATTGATATGC-3'). PCR amplifications registered a sole fragment of approximately 550 bp identical for all *Fusarium* species on 1.5 % agarose gel after proper electrophoresis. The PCR product of the samples showing proper amplification were sent for ITS region sequencing to Chromous Biotech Pvt. Ltd. Bangalore.

The expected 550 bp size of PCR product of ITS region was found to be slightly different after sequencing. The maximum size of sequence was found in *F. proliferatum* (511 bp) followed by *F. graminearum* (510 bp), *F. tricinctum* (502 bp), *F. semitectum* (498 bp), *F. scirpi* (496 bp) and *F. culmorum* (493 bp), while *F. solani* (492 bp) and *F. moniliforme* (492 bp) showed the similar size sequences followed by *F. acuminatum* (491 bp) and *F. oxysporum* (486 bp). However, the minimum size of sequence was reported in case of *F. equiseti* (485 bp).

All the above 11 sequences after complete validation were submitted to the European Molecular Biology Laboratory (EMBL) through their online submission procedure. None of the online available nucleotide databases have sequence of ITS-4 region of *Fusarium*. Therefore, EMBL accepted these sequences and assigned specific accession number to all these sequences. The details of sequences submitted to EMBL database and their accession numbers are given in Table S1 (in the Supplementary Information (SI) section).

Later, the ITS-4 sequences thus obtained for all 11 *Fusarium* species were subjected to BLAST network service, so as to determine the homology. As the BLAST service is free and available online, the nucleotide sequences (ITS-4) were compared (aligned) with all the sequences available with nucleotide databases. Homology search were performed within the non-redundant databases of GeneBank using the BLAST algorithm at NCBI.⁵⁵

The resulting output showed the best similarity matches with the sequences available in databases. The BLAST results reported for all sequences of present study revealed that each sequence of 11 *Fusarium* species have homology with nucleotide sequences of same species present in the databases at different similarity level range between 98-100%. Each of the above tested *Fusarium* species showed the maximum hits with different strains of the same species. BLAST analysis confirmed that all the 11 groups of *Fusarium* species classified on the basis of morphological characters are similar to the identification by molecular markers (ITS rDNA sequence comparison).

Sequence based UPGMA analysis was carried out for the determination of genetic variation among the 11 *Fusarium* species. For the phylogenetic analysis of these species, initially multiple sequence alignment was carried out using a program Clustal-W available online. The alignment file, thus obtained was used for the construction of dendrogram using UPGMA tool of phylogenetic analysis program NTSYS pc. 2.02.

The UPGMA cluster analysis clearly grouped these species into 7 major clusters (Figure 1) and established their relationship of similarity. Genetic relationship calculated in the form of similarity coefficient (Jaccard's coefficients) from the dendrogram showed high level of genetic similarity among all different species of *Fusarium*, which ranges from 0.00 to 0.04.

Cluster analysis obtained from the ITS-4 sequences clearly distinguished all the 11 *Fusarium* species in 7 different main clades. Of the 7 clusters, first clade includes 2 species- *F. solani* and *F. equiseti* having the similarity coefficient of 0.00. The second clade contains *F. tricinctum*

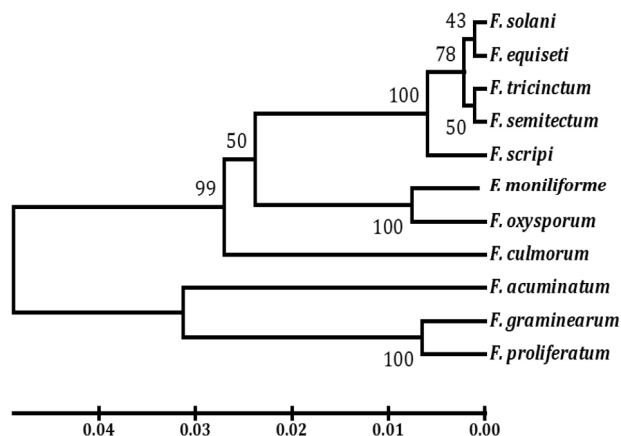


Figure 1. ITS sequence based tree (rectangular) of 11 different species of *Fusarium* constructed using UPGMA. The numbers at branch node indicate the confidence value of bootstrap replications.

and *F. semitectum* which also have similarity coefficient of 0.00 showing that these species are closely related to each other. The third clade represents only *F. scirpi*. The fourth clade includes *F. moniliforme* and *F. oxysporum* having similarity coefficient 0.02. Each of fifth and sixth clusters contain single *F. culmorum* and *F. acuminatum* species respectively. The last and seventh cluster found to have two *Fusarium* species (*F. graminearum* and *F. proliferatum*) having similarity coefficient of 0.01. The sequence based BLAST and phylogenetic analysis is found to be very significant for the rapid identification of *Fusarium* species.

All the above 11 species were screened for the synthesis of silver nanoparticles, which showed potential for the reduction of silver ions to silver nanoparticles. Colour change in the reaction mixture from yellowish to brown (Figure 2) indicates the formation of silver nanoparticles.

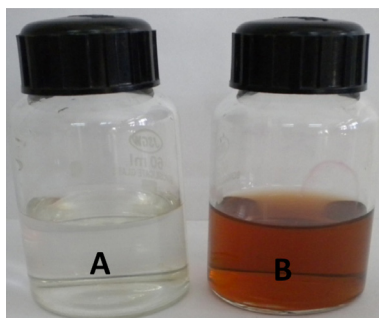


Figure 2. (A) Control (fungal filtrate); (B) colour change of fungal filtrate after treatment with 1 mmol L⁻¹ AgNO₃.

The colour change is due to plasmon resonance in silver nanoparticles. Interestingly in metal nanoparticles like silver, the electrons move freely owing to the close proximity of conduction and valence band.⁵⁶ The collective oscillation of electrons of silver nanoparticles in resonance with the light wave gives rise to a unique Surface Plasmon

Resonance (SPR) absorption band which is also the origin of the observed colour. The absorption strongly depends on the chemical surroundings and particle size.⁵⁷⁻⁶⁰

Silver nanoparticles produced by different *Fusarium* species was characterized by UV-Vis spectrophotometer. All samples showed the absorption peaks at about 420 nm, which is specific for silver nanoparticles (plasmon band) (Figure 3 and Figure S1a-j in the SI section).

It is well known that there is a very close relationship between the UV-Vis light absorbance characteristics, size and shape of absorbate. Only single peak was recorded for each species indicating the formation of spherical nanoparticles. Furthermore, with the increase in the particle size, the optical absorption spectra of metal nanoparticles that are dominated by surface plasmon resonances (SPR) shift towards longer (red-shift) wavelengths.⁶¹

F. oxysporum demonstrated an efficient synthesis of silver nanoparticles with narrow peak (monodispersive) showing blue-shift, which indicates the small sized nanoparticles (Figure 3), while other species showed the broad peaks indicating the formation of polydispersive silver nanoparticles with red-shift (Figure S1a-j). On the basis of UV-Vis spectrophotometric analysis and stability of silver nanoparticles (studied using UV-Vis spectrophotometric analysis), six species, viz., *F. graminearum*, *F. solani*, *F. oxysporum*, *F. culmorum*, *F. scirpi* and *F. tricinctum* were selected for the further characterization (XRD, NTA, TEM, and ZetaSizer).

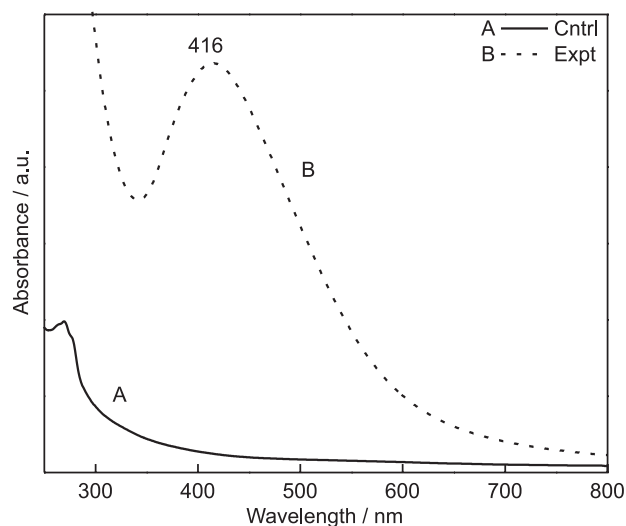


Figure 3. Representative UV-Visible spectra recorded for *Fusarium oxysporum*. (A) Fungal filtrate; (B) fungal filtrate + AgNO₃.

XRD analysis was carried out for all six species of *Fusarium* including *F. graminearum*, *F. solani*, *F. oxysporum*, *F. culmorum*, *F. scirpi*, *F. tricinctum* and the samples produced by the 6 species were observed at

positions 38° , 44° , 66° and 78° of 2θ , depicting the presence of (111), (200), (220) and (311) facets of FCC structure of silver nanoparticles. These values are in agreement with JCPD (Joint Committee on Powder Diffraction, standard file no. 04-0783). Similar pattern of FCC structure was reported for the nanoparticles synthesized from all six *Fusarium* species. Figure 4 showed the powder X-ray diffractometry pattern reported for silver nanoparticles synthesized from *F. oxysporum*.

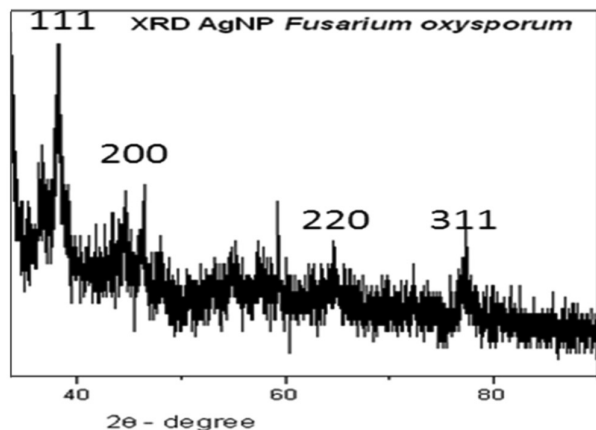


Figure 4. X-ray diffraction pattern of silver nanoparticles synthesized using *F. oxysporum* showing fcc structure.

Nanoparticle tracking and analysis (NTA) was carried using NanoSight LM-20 for all the selected six *Fusarium* species. It is used to measure the dispersion characteristics, i.e. size and distribution. NTA was assessed in-depth due to its ability to measure the size of particles individually on a particle-by-particle basis. NTA allows individual nanoparticles in a suspension to be microscopically visualized and their Brownian motion to be separately but simultaneously analyzed, from which the particle size distribution can be obtained. The average size and concentration of silver nanoparticles recorded from NTA analysis have been shown in Table 1.

Table 1. Average size and concentration of nanoparticles by NTA analysis

S. N.	<i>Fusarium</i> sp.	Average size / nm	Concentration / (particle mL ⁻¹)
1	<i>F. graminearum</i>	42±1.1	1.32 × 10 ¹⁰
2	<i>F. solani</i>	39±1.4	1.02 × 10 ¹⁰
3	<i>F. oxysporum</i>	24±1.5	0.42 × 10 ¹⁰
4	<i>F. culmorum</i>	38±1.5	0.32 × 10 ¹⁰
5	<i>F. scirpi</i>	43±1.9	0.78 × 10 ¹⁰
6	<i>F. tricinctum</i>	45±1.5	2.52 × 10 ¹⁰

S.N.: Serial Number

The small-sized nanoparticles were synthesized by *F. oxysporum* (24 nm) followed by *F. culmorum* (38 nm), *F.*

solani (39 nm), *F. graminearum* (42 nm), *F. scirpi* (43 nm) and *F. tricinctum* (45 nm). Figure S2 shows the particle size distribution histograms. Many earlier reports suggested that NTA is one of the suitable analysis procedures for the determination of size and concentration of nanoparticles.⁶²

It is well known that the metal nanoparticles of size ranging from 2 to 100 nm exhibit strong but broad surface plasmon peak. With the increase in the particle size, the optical absorption spectra of metal nanoparticles that are dominated by surface plasmon resonances (SPR) shift towards longer wavelengths. The position of absorption band also strongly depends upon dielectric constant of the medium and surface-adsorbed species.⁶³ Mock *et al.*⁶⁴ in their study on effects of shape in plasmon resonance of individual colloidal AgNPs concluded that the geometrical shape of a nanoparticle plays an important role in determining the plasmon resonance, while the spectrum red-shifts with increasing particle size.

In the present study, on comparing the absorbance of colloidal silver nanoparticles with their size determined by NTA analysis reveals that with the increase in the particle size, the absorbance spectra shifts towards longer wavelength. Of the 6 *Fusarium* species, the highest absorbance was shown by *F. tricinctum* at 435 nm with largest particle size of 45 nm, while the lowest absorbance was exhibited by *F. oxysporum* with smallest particles size (24 nm). Therefore, in general it can be concluded that larger the particle size, the higher the wavelength for absorbance due to surface plasmon resonance. This clearly indicated that for smaller size particles blue shift, and for larger size of particles red shift in the spectrum was observed with exception of *F. graminearum*.

Further, TEM analysis was also carried out to find out the shape and size of silver nanoparticles produced by six selected *Fusarium* species, which confirmed the spherical shape of synthesized silver nanoparticles. The size of nanoparticles synthesized by all species was in the range of 2-68 nm (Figure 5). Silver nanoparticles synthesized by *F. oxysporum* showed size range 2-42 nm with the smallest average size of 15 nm, while *F. solani* synthesized comparatively larger sized nanoparticles in the range of 9-68 nm with the largest average size of 39 nm amongst the *Fusarium* sps., *F. tricinctum* showed an average size of 20 nm, which is higher than the average size of nanoparticles synthesized by *F. oxysporum*. However, the former showed narrow size dispersion as compared to *F. oxysporum*. Finally, zeta potential was measured to detect the charges acquired by the silver nanoparticles present in medium. High zeta potential indicates the repulsive force and it resists the aggregation of nanoparticles, which helps in the particles stability. In our study, the zeta potential of

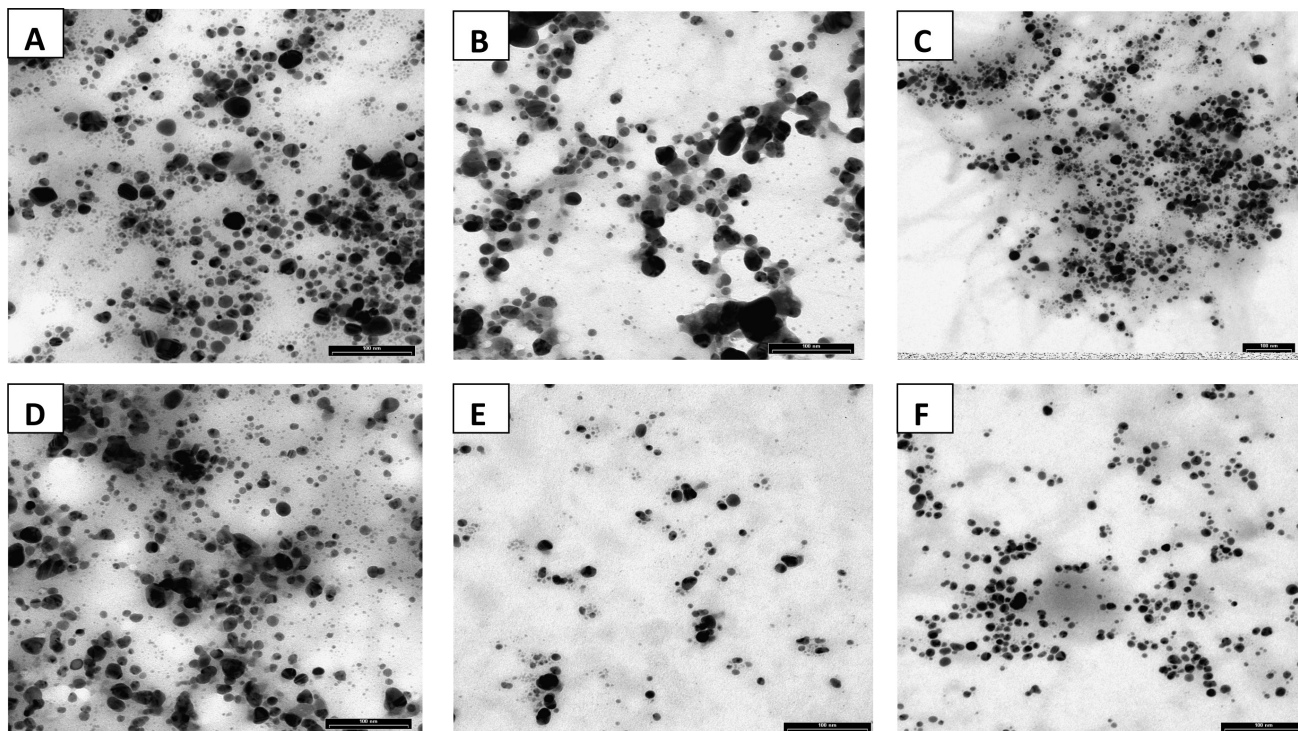


Figure 5. TEM micrographs showing spherical silver nanoparticles synthesized by different *Fusarium* species. (A) *F. graminearum*; (B) *F. solani*; (C) *F. oxysporum*; (D) *F. culmorum*; (E) *F. scirpi*; (F) *F. tricinctum*.

nanoparticles was found to be negative, which might be due to the protein capping on nanoparticles. The greater the zeta potential, the greater the stability of nanoparticles in the colloidal state. The silver nanoparticles formed by *F. tricinctum* showed highest negative zeta potential while thenanoparticles synthesized from *F. culmorum* demonstrated the lowest zeta potential among all species tested (Table 2).

Table 2. Zeta potential reported for silver nanoparticles synthesized from six different *Fusarium* species

S. N.	<i>Fusarium</i> sp.	Zeta potential / mV
1	<i>F. graminearum</i>	-12.4 ± 1.7
2	<i>F. solani</i>	-13.6 ± 1.5
3	<i>F. oxysporum</i>	-15.8 ± 1.4
4	<i>F. culmorum</i>	-10.3 ± 1.5
5	<i>F. scirpi</i>	-12.2 ± 1.4
6	<i>F. tricinctum</i>	-38.3 ± 1.8

S.N.: Serial Number

Conclusions

All the 11 different *Fusarium* species isolated from infected fruits, vegetables and food grains have potential for the formation of silver nanoparticles, which adds to the knowledge about fungal sources that synthesise silver nanoparticles efficiently. Data concerning characterization

of silver nanoparticles revealed that six *Fusarium* species synthesized particles with small size, which indicates their importance in synthesis of novel nanoparticles. Furthermore, the synthesis of silver nanoparticles by *F. graminearum*, *F. scirpi*, and *F. tricinctum* is being reported for the first time.

Supplementary Information

Supplementary Information (data information) is available free of charge at <http://jbcs.sbq.org.br> as PDF file.

Acknowledgement

The authors are thankful to Department of Science and Technology (DST), New Delhi and CNPq Brazil for financial assistance under the framework of Indo-Brazil international Exchange Program. MKR thankfully acknowledges FAPESP for financial support to visit IQ-Universidade Estadual de Campinas, SP, Brazil.

References

1. Maruccio, G.; Cingolani, R.; Rinaldi, R.; *J. Mater. Chem.* **2004**, *14*, 542.
2. Venugopal, G.; Hunt, A.; Alamgir, F.; *Material Matters* **2010**, *5*, 42.

3. Englert, B. C.; *J. Environ. Monit.* **2007**, *9*, 1154.
4. Barreto, J. A.; O'Malley, W.; Kubeil, M.; Graham, B.; Stephan, H.; Spiccia, L.; *Adv. Mater.* **2011**, *23*, H18.
5. Bhattacharyya, A.; Bhaumik, A.; Rani, P. U.; Mandal, S.; Epiidi, T. T.; *Afr. J. Biotechnol.* **2010**, *9*, 3489.
6. Durán, N.; Marcato, P. D.; *Int. J. Food Sci. Technol.* **2013**, *48*, 1127.
7. Perez, H. T.; Castanon, G. M.; *Nanomedicine: NBM* **2008**, *4*, 237.
8. Kumar, A.; Mandal, S.; Selvakannan, P. R.; Parischa, R.; Mandale, A. B.; Sastry, M.; *Langmuir* **2003**, *19*, 6277.
9. Chen, X.; Wu, G.; Chen, J.; Chen, X.; Xie, Z.; Wang, X.; *J. Am. Chem. Soc.* **2011**, *133*, 3693.
10. Chandrasekharan, N.; Kamat, P. V.; *J. Phys. Chem. B* **2002**, *104*, 10851.
11. Mandal, D.; Bolander, M. E.; Mukhopadhyay, D.; Sarkar, G.; Mukherjee, P.; *Appl. Microbiol. Biotechnol.* **2005**, *69*, 485.
12. Nangia, Y.; Wangoo, N.; Goyal, N.; Shekhawat, G.; Suri, C. R.; *Microb. Cell Fact.* **2009**, *8*, 39.
13. Ahmad, A.; Senapati, S.; Khan, M. I.; Kumar, R.; Ramani, R.; Srinivas, V.; Sastry, M.; *Nanotechnology* **2003**, *14*, 824.
14. Namasivayam, S. K. R.; Ganesh, S.; Avimanyu.; *Int. J. Medicobiological Res.* **2011**, *1*, 130
15. Apte, M.; Girme, G.; Bankar, A.; Ravikumar, A.; Zinjarde, S.; *J. Nanobiotechnology* **2013**, *11*, 2.
16. Govindaraju, K.; Basha, S. K.; Ganesh Kumar, V.; Singaravelu, G.; *J. Mater. Sci.* **2008**, *43*, 5115.
17. Narayanan, K. B.; Sakthivel, N.; *Adv. Colloid Interface Sci.* **2011**, *169*, 59.
18. Song, J. Y.; Kwon, E. Y.; Kim, B. S.; *Bioprocess Biosyst. Eng.* **2010**, *33*, 159.
19. Ahmad, A.; Mukherjee, P.; Senapati, D. S.; Mandal, D.; Khan, M. I.; Kumar, R.; Sastry, M.; *Colloids Surf. B: Biointerf.* **2003**, *28*, 313
20. Durán, N.; Marcato, P. D.; Alves, O. L.; De Souza, G. I. H.; Esposito, E.; *J. Nanobiotechnology* **2005**, *3*, 1.
21. Durán, N.; Marcato, P. D.; Souza, G.; Alves, O. L.; Esposito, E.; *J. Biomed. Nanotechnol.* **2007**, *3*, 203.
22. Durán, N.; Marcato, P. D.; Ingle, A.; Gade, A.; Rai, M. In *Progress in Mycology*; Rai, M.; Kövics, G., eds.; Scientific Publishers: Jodhpur, India, 2010, ch. 16, pp. 425.
23. Durán, N.; Marcato, P. D.; Durán, M.; Yadav, A.; Gade, A.; Rai, M.; *Appl. Microbiol. Biotechnol.* **2011**, *90*, 1609.
24. Ingle, A.; Gade, A.; Pierrat, S.; Sonnichsen, C.; Rai, M.; *Curr. Nanosci.* **2008**, *4*, 141.
25. Rai, M.; Yadav, A.; Gade, A.; *Biotechnol. Advan.* **2009**, *27*, 76.
26. Bawaskar, M.; Gaikwad, S.; Ingle, A.; Rathod, D.; Gade, A.; Durán, N.; Marcato, P. D.; Rai, M.; *Curr. Nanoscience* **2010**, *6*, 376.
27. Rai, M. K.; Yadav, A.; Bridge, P.; Gade, A. In *Applied Mycology*; Rai, M.; Bridge, P. D., eds.; CAB International: New York, 2009.
28. Birla, S. S.; Tiwari, V. V.; Gade, A. K.; Ingle, A. P.; Yadav, A. P.; Rai, M. K.; *Lett. Appl. Micro.* **2009**, *48*, 173.
29. Li, G.; He, D.; Qian, Y.; Guan, B.; Gao, S.; Cui, Y.; Yokoyama, K.; Wang, L.; *Int. J. Mol. Sci.* **2012**, *13*, 466.
30. Riddin, T. L.; Gericke, M.; Whiteley, C. G.; *Nanotechnology* **2006**, *17*, 3482.
31. Ahmad, A.; Mukherjee, P.; Mandal, D.; Senapati, S.; Khan, M. I.; Kumar, R.; Sastry, M.; *J. Am. Chem. Soc.* **2002**, *124*, 12108.
32. Seabra, A. B.; Durán, N.; *Curr. Biotechnol.* **2012**, *1*, 287.
33. Bansal, V.; Syed, A.; Bhargava, S. K.; Ahmad, A.; Sastry, M.; *Langmuir* **2007**, *23*, 4993.
34. Durán, N.; Marcato, P. D. In *Nano-Antimicrobials: Progress and Prospects*; Rai, M.; Cioffi, N., eds.; Springer: Verlag Berlin Heidelberg, Germany, 2012, part 3, pp. 337.
35. Bansal, V.; Rautaray, D.; Bharde, A.; Ahire, K.; Sanyal, A.; Ahmad, A.; Sastry, M.; *J. Mater. Chem.* **2005**, *15*, 2583.
36. Duncan, T. V.; *J. Colloid Interface Sci.* **2011**, *363*, 1.
37. Ilic, V.; Saponjic, Z.; Vodnik, V.; Lazovic, S.; Dimitrijevic, S.; Jovancic, P.; Nedeljkovic, J. M.; Radetic, M.; *Ind. Eng. Chem. Res.* **2010**, *49*, 7287.
38. El-Rafie, M. H.; Shaheen, T. I.; Mohamed, A. A.; Hebeish, A.; *Carbohydr. Polym.* **2012**, *90*, 915.
39. Marcato, P. D.; Nakasato, G.; Brocchi, M.; Melo, P. S.; Huber, S. C.; Ferreira, I. R.; Alves, O. L.; Durán, N.; *J. Nano Res.* **2012**, *20*, 69.
40. Kokura, S.; Handa, O.; Takagi, T.; Ishikawa, T.; Naito, Y.; Yoshikawa, T.; *Nanomedicine: NBM*, **2010**, *6*, 570.
41. Abdi, G.; Salehi, H.; Khosh-Khui, M.; *Acta Physiol. Plant.* **2008**, *30*, 714.
42. Savage, N.; Diallo, M. S.; *J. Nanopart. Res.* **2005**, *7*, 331.
43. Sierra, J. F. H.; Ruiz, F.; Pena, D. C. C.; Gutierrez, F. M.; Martinez, A. E.; Guillen, A. J. P.; Perez, H. T.; Castanon, G. M.; *Nanomedicine: NBM* **2008**, *4*, 237.
44. Devi, L. S.; Joshi, S. R.; *Mycobiology* **2012**, *40*, 27.
45. Syed, A.; Ahmad, A.; *Spectrochim. Acta A* **2013**, *12*, 47.
46. Knetsch, M. L. W.; Koole, L. H.; *Polymers* **2011**, *3*, 340.
47. Soni, N.; Prakash, S.; *Parasitol. Res.* **2012**, *111*, 2091.
48. Gade, A.; Ingle, A.; Whiteley, C.; Rai, M.; *Biotechnol. Lett.* **2010**, *32*, 593.
49. Rai, M. K.; Deshmukh, S. D.; Ingle, A. P.; Gade, A. K.; *J. Appl. Microbiol.* **2012**, *112*, 841.
50. Lara, H. H.; Ayala-Núñez, N. V.; Turrent, L. C. I.; Padilla, C. R.; *World J. Microbiol. Biotechnol.* **2012**, *26*, 615.
51. Seifert, K.; *Agriculture and Agri-Food Canada* **1996**, *1*, 65.
52. Leslie, J. F.; Summerell, B. A.; *The Fusarium Laboratory Manual*, 3rd ed.; Blackwell: Ames, IA, USA, 2006.
53. Nelson, P. E.; Dignani, M. C.; Anaissie, E. J.; *Clin. Microbiol. Rev.* **1994**, *7*, 479.
54. Alexopoulos, C. J.; Mims, C. W.; Blackwell, M.; *Introductory Mycology*, 4th ed.; John Wiley & Sons: Singapore, 1996.

55. <http://blast.ncbi.nlm.nih.gov/Blast.cgi> accessed in September, 2013.
56. Nath, S. S.; Chakdar, D.; Gope, G.; *Nanotrends* **2007**, 2, 1.
57. Link, S.; El-Sayed, M. A.; *Annu. Rev. Phys. Chem.* **2003**, 54, 331.
58. Noginov, M. A.; Zhu, G.; Bahoura, M.; Adegoke, J.; Small, C.; Ritzo, B. A.; Drachev, V. P.; Shalaev, V. M.; *Appl. Phys. B* **2007**, 86, 455.
59. Litvin, V. A.; Minaev, B. F.; *Spectrochim. Acta A* **2013**, 108, 115.
60. Litvin, V. A.; Galagan, R. L.; Minaev, B. F.; *Colloids Surf. A Physicochem. Eng. Asp.* **2012**, 414, 234.
61. Shafeev, G. A.; Freysz, E.; Bozon-Verduraz, F.; *Appl. Phys. A* **2004**, 78, 307.
62. Raheman, F.; Deshmukh, S.; Ingle, A.; Gade, A.; Rai, M.; *Nano Biomed. Eng.* **2011**, 3, 174.
63. Xia, Y.; Halas, N. J.; *MRS Bulletin* **2005**, 30, 338.
64. Mock, J. J.; Barbic, M.; Smith, D. R.; Schultz, D. A.; Schultz, S.; *J. Chem. Phys.* **2002**, 116, 6755.

Submitted: May 22, 2013

Published online: October 9, 2013

FAPESP has sponsored the publication of this article.

Supplementary Information

Screening of Different *Fusarium* Species to Select Potential Species for the Synthesis of Silver Nanoparticles

Swapnil C. Gaikwad,^a Sonal S. Birla,^a Avinash P. Ingle,^a Aniket K. Gade,^{a,e}
Priscyla D. Marcato,^{b,c} Mahendra Rai^{*,a,c} and Nelson Duran^{c,d}

^aDepartment of Biotechnology, SGB Amravati University, Amravati-444 602, Maharashtra, India

^bInstitute of Chemistry, Biological Chemistry Laboratory, Universidade Estadual de Campinas, CP 6154, 13083-970 Campinas-SP, Brazil

^cNanobiolab, Faculty of Pharmaceutical Sciences of Ribeirão Preto, Universidade de São Paulo, Av. do Café, s/n, 14040-903 Ribeirão Preto-SP, Brazil

^dCenter of Natural and Human Sciences, Universidade Federal do ABC, Rua Santa Adélia, 166, 09210-170 Santo André-SP, Brazil

^eDepartment of Biology, Utah State University, 84322 Logan-UT, USA

Table S1. List of ITS sequences of *Fusarium* species and their GeneBank accession numbers

S. N.	<i>Fusarium</i> species	EMBL GeneBank accession No.
1	<i>F. semitectum</i>	FR851230
2	<i>F. oxysporum</i>	FR851229
3	<i>F. equiseti</i>	FR851233
4	<i>F. acuminatum</i>	FR851231
5	<i>F. proliferatum</i>	FR851236
6	<i>F. moniliforme</i>	FR851235
7	<i>F. tricinctum</i>	FR851237
8	<i>F. graminearum</i>	FR851234
9	<i>F. culmorum</i>	FR851232
10	<i>F. solani</i>	FR878062
11	<i>F. scirpi</i>	FR878061

S.N.: Serial Number

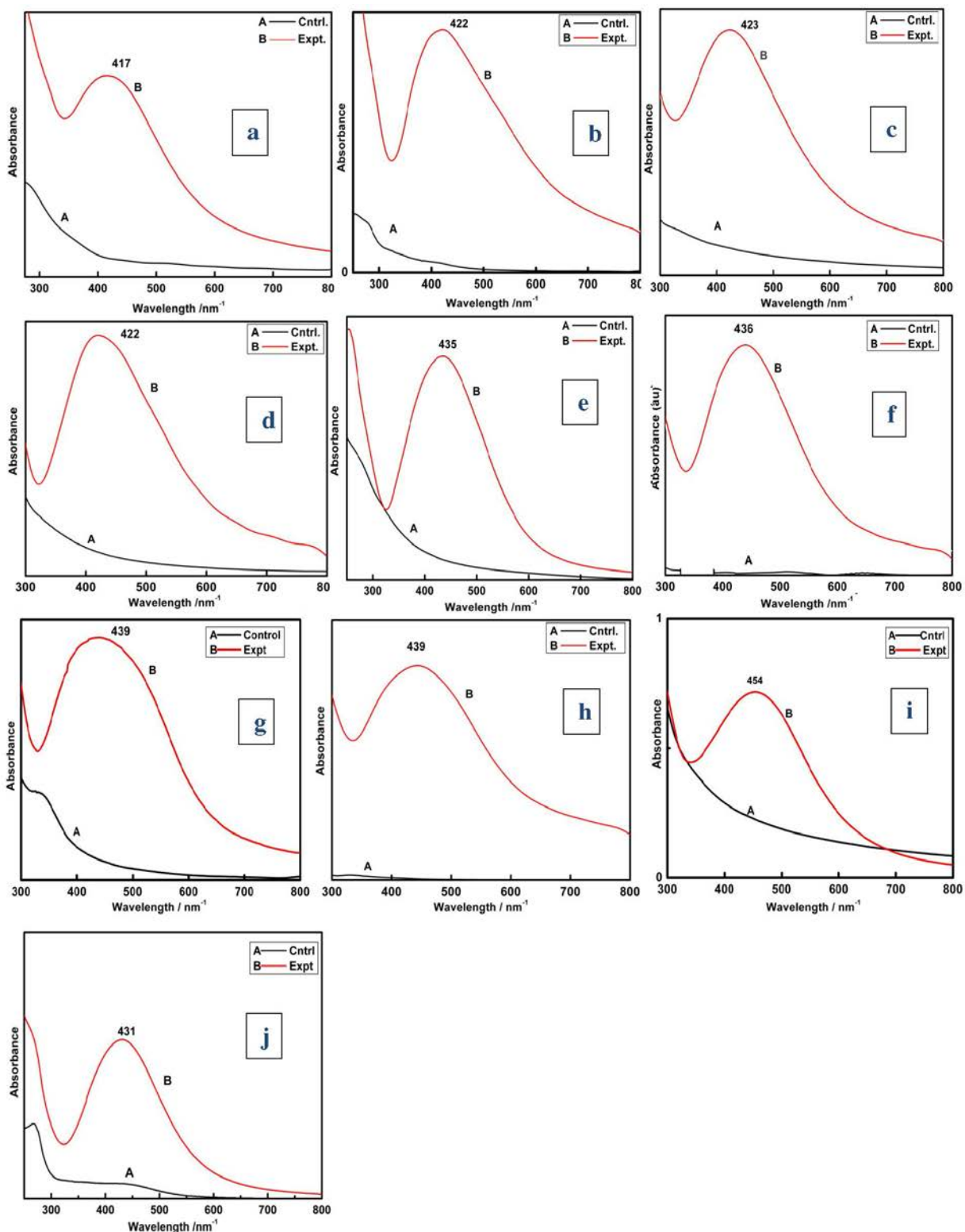


Figure S1. UV-Visible spectra recorded for 10 different *Fusarium* species (a. *F. graminearum*, b. *F. solani*, c. *F. culmorum*, d. *F. scirpi*, e. *F. tricinctum*, f. *F. acuminatum*, g. *F. semitectum*, h. *F. proliferatum*, i. *F. equiseti*, j. *F. moniliforme*). A- Cntrl (fungal filtrate), B- Expt (Fungal filtrate + AgNO_3).

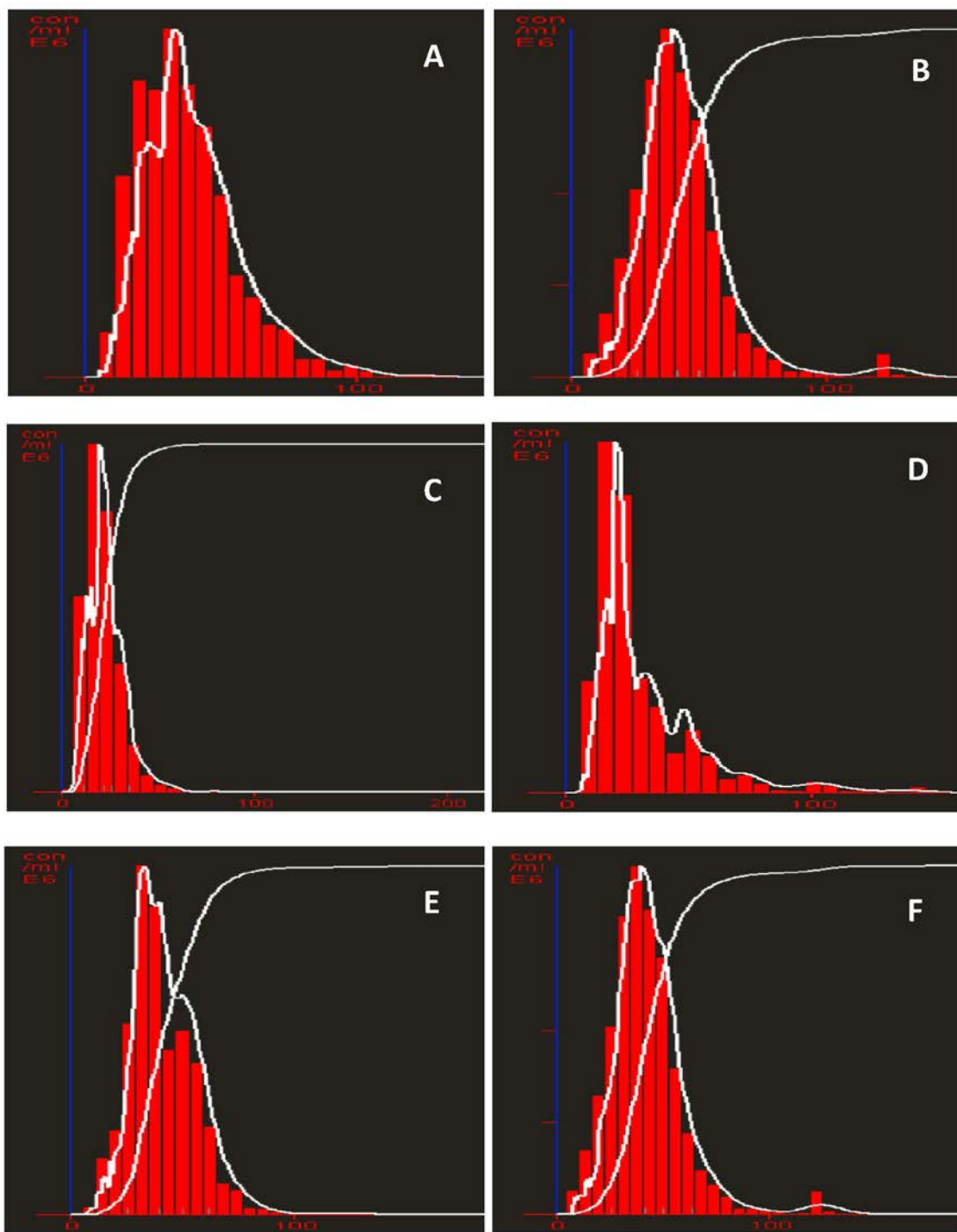


Figure S2. Particle size distribution histograms obtained from NTA analysis of silver nanoparticles synthesized by different *Fusarium* species. (A) *F. graminearum*; (B) *F. solani*; (C) *F. oxysporum*; (D) *F. culmorum*; (E) *F. scirpi*; (F) *F. tricinctum*.